Harvesting the volatility smile: A Dynamic Nelson Siegel approach

Abstract

While there is a large literature on modeling volatility smile in options markets, almost all such studies are eventually focused on the forecasting performance of the model parameters and not on the applicability of the models in a trading environment. Drawing on the analogy of a volatility smile as interest rate term structure, we evaluate the performance of the Dynamic Nelson Siegel approach to model the dynamics of volatility smile in a trading environment against competing alternatives. Based on rank ordering of options identified by model-based mispricing, our trading strategy is to go long the options in the upper deciles and going short the options in the lower deciles. We show that, in general, dynamic models outperform their static counterparts, with the worst dynamic model outperforming the best static model in terms of percentage of positive returns from the trading portfolios and the Sharpe ratio. Specifically, we find that the Dynamic Nelson Siegel model consistently outperforms all other competing specifications on most of our selected criteria.

Keywords: Dynamic Nelson Siegel, Equity derivatives, Kalman Filter, State space models, Options market, Volatility smile
JEL: C14; C32; C52; G12; G13

1. Introduction

There is a growing literature on understanding the behaviour of volatility smile in option markets, the name given to the commonly observed empirical relationship between implied volatility (IV) and option strike. In the last decade, using data from economies with liquid option markets, there have been many articles published on the modeling of volatility smile, as well as on its applications in the larger literature on option pricing, financial engineering and risk management (Cont and Fonseca, 2002; Hagan et al., 2002; Carr and Wu, 2003; Christoffersen et al., 2009; Taylor et al., 2010; Grnborg and Lunde, 2016; Garca-Machado and Rybczyski, 2017; Wong and Heaney, 2017; Jain et al., 2019; Kim et al., 2020; Kim, 2021; Franois and Stentoft, 2021a).

The importance of having a systematic approach to modeling volatility smile cannot be overemphasized – option traders are known to quote not option prices but volatility implied by them during trading (Reiswich and Wystup, 2009; Wong and Heaney, 2017), making IV an important forward-looking measure of financial market's view of uncertainty and risk aversion over the life of an option contract (Koopman et al., 2005; Jin et al., 2012; Park et al., 2019). Options are traded for various strikes, and each strike provides additional information about market participant's view of the prevailing uncertainty and movement of future stock returns and volatility. Given the option price, in terms of the Black (1976) formula, IV is written as an inverse function:

$$\text{Implied volatility} \equiv \sigma_{\text{IV}} = \text{Option price}^{-1}_{\text{Black}}\big(V, F, K, r, \tau\big)$$

where V, F, K, r, and τ respectively denote the option price, price of futures contract with same maturity as the option, strike price, the risk-free rate, and the time to maturity.

Given the empirically established nature of volatility smile across markets, asset classes and geographies (for a survey, see Derman and Miller, 2016; Kearney et al., 2019) a working model for IV becomes important for a variety of reasons. Firstly, and possibly most importantly, it allows option traders to implement trading strategies given their view on the evolution of volatility smile (Kim et al., 2020). Secondly, a model for the volatility smile allows for extracting the market implied risk-neutral probability distribution of future price movements (Malz, 1997; Jackwerth, 2004; Hayashi, 2020). Finally, the ability to price over-the-counter or exotic equity derivatives requires volatility smile as an input to stochastic volatility models, to ensure that the model-dependent price of any exotic option and the associated hedging strategy are consistent with the prices of prevailing plain vanilla option prices (Dupire, 1994; Rebonato, 2004; Wong and Heaney, 2017; Gatheral et al., 2020).

This paper contributes to the stream of literature on modeling volatility smile by showing the superiority of dynamic models of IV for implementing trading strategies using stock options data from the National Stock Exchange of India (NSE). The reason for choosing data from NSE are two-fold: i) it is one of the few markets worldwide with a liquid stock options market, consistently ranking among the largest options market globally by volume (World Federation of Exchanges, 2021), and ii) unlike most developed country options markets,

NSE also has liquid futures contracts simultaneously with liquid options on the same stock, allowing us to directly use the Black (1976) formula to find implied volatility without needing to estimate stock-wise dividend yield (Jain et al., 2019).

We draw on the analogy of a volatility smile as interest rate term structure (Derman et al., 1996; Rogers and Tehranchi, 2010), and use a popular approach to fit the term structure in fixed income markets called the Dynamic Nelson Siegel (DNS) model (Diebold and Li, 2006) to fit IV as a function of delta dynamically. The use of the Diebold and Li (2006) approach to model the time evolution of volatility is not new. Starting from the work of Chalamandaris and Tsekrekos (2011), many researchers have used their flexible approach to model volatility surface across markets (Chalamandaris and Tsekrekos, 2014; Guo et al., 2014) and asset classes (Kearney et al., 2019). All these papers, however, use the Diebold and Li (2006) specification to only model the *time dimension* of the volatility surface and not for modeling the dynamics of the smile itself. Also, most of these studies are eventually focused on the forecasting performance of the model parameters and not on their applicability or use in a trading environment.

There are three main concerns in using static models for fitting the volatility smile. Firstly, there is no way to ensure that smile evolution is economically reasonable, and because parameters are estimated separately for each day, the fitted smile can vary wildly over consecutive days. Secondly, even in liquid option markets, not all instruments or option strikes are equally liquid (World Federation of Exchanges, 2021), and price of illiquid options can often be distorted. This is similar to the phenomenon of not all Government bonds being equally liquid in fixed-income markets (Cortazar et al., 2007; Nagy, 2020). Thirdly, and specific to the use of lower-order polynomials in fitting volatility smile (Jain et al., 2019), quadratic models assume a symmetry which is at odds with the observed downward sloping relationship between IV and delta (often called a skew or a smirk) for stock options (Zhang and Xiang, 2008).

The use of dynamic state space models addresses all of these concerns. By design, the DNS approach estimates the whole panel of observations together by explicitly incorporating the time dynamics of the underlying factors. This allows for aggregating trading information over a longer period in a theoretically consistent manner, so the distorted prices pose less of a problem and the specification is flexible enough to capture smirks at the same time. Finally, with a larger sample of observations available and a reasonable dynamics imposed on the parameters by construction, the parameter evolution is naturally smoother. In terms of a state space interpretation of the model, our study is closest to that of Chen et al. (2018) who apply the adaptive version of DNS (Chen and Niu, 2014) which successively estimates the model parameters over optimal subsamples of varying lengths.

We show that our implementation based on the DNS model estimated using the Kalman Filter outperforms other comparable candidates in terms of profit generated from trading strategies. In our horse race, we consider four specifications: the DNS model estimated for the full sample, a static Nelson Siegel (SNS) model estimated separately for each day in the sample, and similarly for the dynamic and static versions of a quadratic polynomial

used by Jain et al. (2019) on the same NSE data in an earlier study. The Dynamic Nelson Siegel model consistently outperforms the other three specifications on most of our selected criteria. Although static models provide marginally better in-sample fit than their dynamic counterparts, their performance is marred by highly unstable factor estimates over time.

The main contribution of this study is to evaluate the utility of popular competing models from the perspective of an options trading desk. We create delta and vega-neutral portfolios of option contracts by buying/selling undervalued/overvalued options (as implied by the models) for 100 different stocks in each expiration cycle. The DNS model performs the best with a 65% win rate (percentage of positive returns in the sample), a 104% mean annual return, and with a Sharpe ratio of 0.13. Using a one-sided paired Wilcoxon Rank test, we also demonstrate that the returns generated by the DNS model are statistically greater than that of competing models at 99% confidence interval. Our results are robust for stocks across industries and expiration cycles.

We also demonstrate that the return generated by the trading strategy is not driven by portfolio exposure to other systematic risk factors relevant to the options market. Given that our portfolios throughout are delta and vega-neutral by design, we regress portfolio return on other relevant option Greeks, including theta, rho, gamma, vanna and vomma and find that none of these Greeks have significant explanatory power for the portfolio returns, suggesting trading returns are driven primarily by the mispricing captured by the DNS model.

Our results also provide some interesting insights about the attributes of our two class of models. On the majority of metrics, dynamic models outperform their static counterparts, with the worst dynamic model outperforming the best static model in terms of the win rate. The comparison between the SNS and quadratic models is more nuanced. In their static avatars, the more parsimonious quadratic model does distinctly better, whereas the more flexible DNS model is superior in a dynamic setting. The lesson here is that a more flexible model needs more data to be effective.

The rest of the paper is structured as follows. Section 2 reviews the related literature and describes our research questions. Section 3 describes the data, and section 4 presents our modeling approach and the estimation methodology. Section 5 discusses the results and presents our main findings. Finally, section 6 concludes.

2. Literature review and research questions

The original Black-Scholes approach to option pricing (Black and Scholes, 1973) was based on the principle of no-arbitrage using the ideas of dynamic replication and a self-financing strategy, and getting to the Black-Scholes formula required many assumptions, including, and most importantly, that of constant volatility (Merton, 1973). In the early 1990s, however, Rubinstein (1994) documented that since the late 1980s, out-of-the-money (OTM) put options on the S&P500 index have consistently traded at a higher prices compared to equivalent OTM call options. In terms of IV, this translates into a higher IV for OTM put

options compared to that for OTM call options, resulting in what has now come to be known as volatility smile.

The theoretical explanations for the existence of a volatility smile include the leverage effect (Black, 1976), increased risk aversion and hedging demand for put options in times of market stress (Franke et al., 1998; Bollen and Whaley, 2004) and a compensation for bearing short-run variance risk (Vogt, 2016). Over time, the existence of volatility smile has been documented in other equity options markets globally (Dennis and Mayhew, 2002; Foresi and Wu, 2005), including the Indian options market (Jain et al., 2019). Figure 1 provides a snapshot of a volatility smile for a sample stock (ticker RELIANCE) as on January 1, 2020.

[Insert Figure 1 about here]

Given the importance of volatility for financial engineering and risk management, modeling volatility smile has been one of the most prolific areas of research within option pricing. The literature on modifying the Black-Scholes model to capture volatility smile has evolved in three broad directions. The first strand attempts to capture the smile using stochastic volatility (SV) models within a no-arbitrage setting, with some of the early popular papers including Hull and White (1987), Stein and Stein (1991) and Heston (1993). They have been found to be particularly useful for pricing path-dependent derivatives (Kou and Wang, 2004, and references therein). In a different context, SV models have also been used by studies who take a general equilibrium approach to option pricing (Guidolin and Timmermann, 2003), though these have been found to only limited empirical success (for a review, see Bedendo and Hodges, 2009).

The second strand on local volatility (LV) models, developed originally by practitioners, modified the Black-Scholes approach by defining volatility as a deterministic function of the underlying stock price and time (Dupire, 1994; Derman and Kani, 1994). Their attractiveness stems from their internal consistency, particularly in their ability to fit prevailing prices of plain vanilla call and put options, making them popular for pricing exotic options (Rebonato, 2004). However, after Hagan et al. (2002) identified that the dynamics of the market smile predicted by LV models varied significantly from the market observed behaviour of the smile, the use of pure LV models has almost ended, and popular models for pricing exotic options today include at least some SV component, effectively leading to merging of models in the first two strands in practice (Rebonato et al., 2009).

The third strand, and the one that has seen the most development in empirical finance recently, involves the use of atheoretical models. These effectively constitute statistical methods that describe the shape of the smile parametrically or non-parametrically, often using unobservable latent factors (Dumas et al., 1998). The different approaches to modeling volatility smile this way in the more modern literature range from use of polynomials (Zhang and Xiang, 2008; Le and Zurbruegg, 2014; Choi et al., 2015; Sui et al., 2020; Kim, 2021; Yue et al., 2021) to use of SV models (Franois and Stentoft, 2021a) to use of semi-parametric methods (Fengler and Hin, 2015, and references therein) and neural networks (Liu et al., 2021). In a recent study with a detailed review of the related literature, Kim (2021) concludes

that such atheoretical models (the author calls them ad hoc Black-Scholes models) are "...the best alternative to mathematically sophisticated option-pricing models given its simplicity of implementation." A study which is methodologically closest to ours, Chen et al. (2018), also acknowledges that "...structured parametric forecasting models achieve superior out-of-sample results."

The literature on volatility smile goes beyond just exploring the relationship between IV and strike or delta. For markets with liquid long-maturity options, researchers have also looked at both the pure term structure of volatility (the time dimension) as well as the volatility surface – the mapping of IV with respect to both strike and time to maturity. Some examples of such studies include Chalamandaris and Tsekrekos (2011), Guo et al. (2014), Chalamandaris and Tsekrekos (2014), Guo et al. (2018), Kearney et al. (2019, and references therein) and Kim et al. (2020). Since liquidity in stock options in India is restricted to those with short maturity, exploring the time dimension or the volatility surface is outside the scope of our study. Even so, the literature and the methodological approach used to model the time dimension and the volatility surface remains quite relevant for us, as many such recent studies use the Diebold and Li (2006) approach, the one that we also use.

The interpretation of a volatility smile as a schedule of IV for varying strikes in options markets – similar to the schedule of interest rates for varying maturities in bond markets – is a powerful idea (Derman et al., 1996; Rogers and Tehranchi, 2010; Derman and Miller, 2016) and something we exploit to model the behaviour of volatility smile in our study. In particular, we use a popular approach to fit the term structure in fixed income markets called the DNS model (Diebold and Li, 2006) to fit IV as a function of delta dynamically. While DNS has been used to model volatility surface across markets (Chalamandaris and Tsekrekos, 2014; Guo et al., 2014) and asset classes (Kearney et al., 2019), the focus in those studies has invariably been on using the Diebold and Li (2006) specification to only model the time dimension of the volatility surface and not for modeling the dynamics of the smile itself. Also, all the above cited studies are eventually focused on the forecasting performance of the model parameters and not on their applicability or use in trading. To our knowledge, there is no other study in the literature which has used our approach to model the time dynamics of volatility smile with respect to option delta in a trading environment.

Our first research question follows directly from the literature reviewed above: do dynamic models of IV perform better or worse than their static counterparts in terms of profit from a trading strategy after accounting for transaction costs? We address this question in the context of both the DNS model of Diebold and Li (2006) as well as the quadratic polynomial approach of Malz (1997) as implemented by Jain et al. (2019). Our second research question relates to the choice of the model itself: does the DNS model perform better or worse than the quadratic polynomial approach?

In a recent study, Agarwalla et al. (2021b) showed that as COVID-19 spread through the economy, the option implied risk-neutral density responded differently across sectors. There is also evidence that there is an idiosyncratic component of information content of IV, with stocks with a higher trading volume containing more information (Sui et al., 2020). Since

our sample includes the onset and spread of COVID-19 in India, our third and final research question relates to determinants of performance of the trading strategy across options on stocks belonging to different sectors of the economy through the spread of COVID-19.

3. Data

We use stock options data from NSE, one of the few markets worldwide with a liquid stock options market along with a simultaneously liquid stock futures market, consistently ranking among the largest options market worldwide (World Federation of Exchanges, 2021). The existence of matching liquid futures contracts allows us to directly use the Black (1976) formula to find IV without needing to estimate stock-wise dividend yield (Jain et al., 2019).

As on date, NSE has more than 150 stock options (SSOs) listed for trading, but not all are equally liquid. To ensure that our results are not affected by highly illiquid contracts, we select top 100 SSOs sorted by trading volume for our purpose (the full list used in the sample is given in table A.1. The sample period is January 1 to December 24, 2020.

Given our focus on implementing our models for trading strategies, only near-month options data are used, and to avoid issues arising from expiration day effects (Bollen and Whaley, 1999) we remove all data with less than five days before the expiry date. Following Franois and Stentoft (2021b), we also remove all observations which violate the option bounds, and following Mixon (2009), we only consider those stock option days where at least five unique options have been traded. Overall, this leaves us with a final sample consisting of a total of 501,697 daily observations. Table 1 presents a summary of the observations across delta for call (left panel) and put (right panel) options.

As is now common in the literature, we convert delta of the put option into delta of the corresponding call option to make the range of delta in $(0, 1]$ throughout. Our sample period also includes the COVID-19 shock in March 2020. Panel A of Table 1 provides the summary of the full sample, while panel B provides the summary of the subsample around the spread of COVID-19 in March, 2020. Column 'N' presents the monthly average of number of observations, 'Bid-ask Spread (%)' presents average bid-ask spread divided by option price in percentage terms, 'Volume' presents average monthly traded volume, and 'N(trades)' represents the average monthly number of trades. For the risk-free rate input to the Black (1976) formula, the implicit yield at cut-off price of 91-day Treasury bill published by the Reserve Bank of India is used. Finally, for studying determinants of profit from trading strategy through the spread of COVID-19, following Agarwalla et al. (2021b), we classify the stocks into eleven unique industries based on the Global Industry Classification Standard (GICS) (table A.1 provides the classification).

[Insert Table 1 about here]

4. Modeling volatility smile using the Dynamic Nelson Siegel approach

The original Nelson Siegel (NS) model dates back to the 1980s (Nelson and Siegel, 1987), and with its parsimony and intuitive interpretation of model parameters, it has been one

of the most popular choice of models with central banks and practitioners to fit the term structure of interest rates. The NS model assumes that the instantaneous forward rate is the solution to a second-order differential equation with two equal roots. The resulting spot rate or zero-coupon yield from the model is given by:

$$y(\tau) = \beta_0 + \beta_1 \left(\frac{1 - e^{-\lambda\tau}}{\lambda\tau} \right) + \beta_2 \left(\frac{1 - e^{-\lambda\tau}}{\lambda\tau} - e^{-\lambda\tau} \right) \tag{1}$$

Diebold and Li (2006) extended the model into a dynamic setting by allowing the NS parameters to vary over time. Referred to as the Dynamic Nelson Siegel model, its popularity has only increased since (for a recent survey, see Kumar and Virmani, 2022). The dynamics of the spot rate in the DNS model is given by:

$$y_t(\tau) = \beta_{0,t} + \beta_{1,t} \left(\frac{1 - e^{-\lambda\tau}}{\lambda\tau} \right) + \beta_{2,t} \left(\frac{1 - e^{-\lambda\tau}}{\lambda\tau} - e^{-\lambda\tau} \right) \tag{2}$$

where, y_t is the zero-coupon yield at time t with maturity τ, and $\beta_{0,t}$, $\beta_{1,t}$, $\beta_{2,t}$ are often referred to as 'factor loadings' (Nelson and Siegel, 1987). Their behaviour is such that $\beta_{0,t}$ is constant across maturities, $\beta_{1,t}$ is decreasing across maturities, and $\beta_{2,t}$ is hump-shaped, with the parameter λ determining the location of the hump. This structure has been found to be flexible enough to fit different shapes of the yield curve (Diebold and Li, 2006).

Alexander (2001) showed that similar to the term structure, the three principal components of volatility can also be understood in terms of the level, slope and the curvature of volatility smile. In the literature on modeling volatility smile, however, the DNS model has only been predominantly used to model the volatility term structure, with examples including Chalamandaris and Tsekrekos (2011), Guo et al. (2014), Chalamandaris and Tsekrekos (2014), Guo et al. (2018), Kearney et al. (2019, and references therein) and Kim et al. (2020).

Following Alexander (2001) and the analogy drawn by Derman et al. (1996), Rogers and Tehranchi (2010) and Derman and Miller (2016), we use the DNS approach to model the dynamics of volatility smile in our study. To our knowledge, no other study in the literature has taken this approach to modeling the dynamics of the smile. The study closest to ours, methodologically, is that of Chen et al. (2018) who apply the Adaptive DNS approach of Chen and Niu (2014) to model the term structure of volatility smile.

For reasons explained in Agarwalla et al. (2021b), we model volatility smile with respect to option delta (Δ). In particular, analogous to a model for the term structure of interest rates, our model specification for IV as a function of delta ($y_t(\Delta)$) is the following:

$$y_t(\Delta) = \beta_{0,t} + \beta_{1,t} \left(\frac{1 - e^{-\lambda\Delta}}{\lambda\Delta} \right) + \beta_{2,t} \left(\frac{1 - e^{-\lambda\Delta}}{\lambda\Delta} - e^{-\lambda\Delta} \right) + \epsilon_t \tag{3}$$

Depending on the context, ϵ_t or ϵ denote the error terms throughout.

As mentioned earlier, in our horse race of models, we compare profits from a trading strategy based on the DNS model with three alternatives: i) its static avatar, the static Nelson Siegel model (SN), ii) the quadratic polynomial approach of Malz (1997) as implemented by Jain et al. (2019), which we refer to as the static quadratic (SQ) model:

$$y(\Delta) = a\Delta^2 + b\Delta + c + \epsilon \tag{4}$$

and, iv) its dynamic version, which we call the Dynamic Quadratic (DQ) model:

$$y_t(\Delta) = a_t\Delta^2 + b_t\Delta + c_t + \epsilon_t \tag{5}$$

For the static models, the estimation is relatively straight forward, and we estimate the parameters for each day independently by minimizing the weighted sum of the square of the estimation error as:

$$\min \sum_{i=1}^{N} \omega_i \times \left(\sigma_{IV,i} - \widehat{\sigma}_{\text{model},i}(\beta, \Delta)\right)^2 \tag{6}$$

where, as defined earlier, $\sigma_{IV,i} = \text{Option price}^{-1}_{\text{Black},i}\big(V_i, F_i, K_i, r, \tau_i\big)$, $\widehat{\sigma}_{\text{model},i}(\beta, \Delta)$ is the predicted implied volatility from a given model with the parameter vector β. Given the large variation in terms of trading volume and liquidity across option strikes, we incorporate the heterogeneity of the trading volume in the estimation by assigning different weights to the observation measured by the natural logarithm of trading volume, i.e. we set $\omega_i = \log(\text{trading volume}_i)$.

4.1. Estimation of the Dynamic Nelson Siegel and Quadratic models

We cast both our dynamic models in a state space framework and estimate them using the approach laid out in Kumar and Virmani (2022). We describe the steps for estimation for the DNS model here. The approach for estimating the DQ model is analogously identical.

As in Diebold and Li (2006), the three parameters in the DNS ($\beta \equiv (\beta_0, \beta_1, \beta_2)$) model are assumed to follow a Vector Autoregressive process of order 1 or VAR(1). Extending equation 3 earlier, our state space specification for DNS is:

$$\begin{aligned} y_t(\Delta) &= \beta_{0,t} + \beta_{1,t}\left(\frac{1-e^{-\lambda\Delta}}{\lambda\Delta}\right) + \beta_{2,t}\left(\frac{1-e^{-\lambda\Delta}}{\lambda\Delta} - e^{-\lambda\Delta}\right) + \epsilon_t \qquad \text{Measurement equation} \\ \beta_t &= \mathbf{C} + \mathbf{A}\beta_{t-1} + \eta_t \qquad \text{State equation} \end{aligned} \tag{7}$$

where y_t is the observed IV, Δ is the corresponding call delta, and $\beta_t \equiv \{\beta_{0,t}, \beta_{1,t}, \beta_{2,t}\}$ is the vector of time varying NS parameters. The constant vector $\mathbf{C}$ and the matrix $\mathbf{A}$ together define the VAR process. In the language of state space models, ϵ_t captures the measurement error and η_t the state error, with their joint distribution assumed to be Normal/Gaussian:

$$\begin{pmatrix}\epsilon_t\\ \eta_t\end{pmatrix} \sim N\left[\begin{pmatrix}0\\ 0\end{pmatrix}, \begin{pmatrix}H_t & 0\\ 0 & Q_t\end{pmatrix}\right] \tag{8}$$

The standard approach for the estimation of a linear state space model with Gaussian errors is the use of the Kalman Filter and maximum likelihood. The Kalman filter recursively updates the mean and variance of the state vectors. First, the state mean and covariance are initialized at the values of their unconditional mean and covariance respectively:

$$E(\beta_0|\mathcal{F}_0) = E(\beta_0), \quad \Sigma(\beta_0|\mathcal{F}_0) = \Sigma(\beta_0) \tag{9}$$

The update equations for conditional mean and covariance from time $k-1$ to k follow well-defined recursions. At every step of the recursion, the Kalman filter predicts the conditional mean and variance of the measurement variable (y_k) using the updated conditional mean of the state vector. Calling $\mathbf{F}$ as the NS loading of the factors, the main recursions are:

$$\begin{aligned}
E(\beta_k|\mathcal{F}_{k-1}) &= \mathbf{C} + \mathbf{A}E(\beta_{k-1}|\mathcal{F}_{k-1})\\
\Sigma(\beta_k|\mathcal{F}_{k-1}) &= \mathbf{A}\Sigma(\beta_{k-1}|\mathcal{F}_{k-1})\mathbf{A^T} + Q_t\\
E(y_k|\mathcal{F}_{k-1}) &= \mathbf{F}E(\beta_k|\mathcal{F}_{k-1})\\
\Sigma(y_k|\mathcal{F}_{k-1}) &= \mathbf{F}\Sigma(\beta_k|\mathcal{F}_{k-1})\mathbf{F^T} + H_t
\end{aligned} \tag{10}$$

Finally, ζ_k is the prediction error vector measured as difference between y_k and its conditional expectation, and the Kalman filter algorithm uses ζ_k to update the inference about the unobserved state vector by revising its conditional expectation and variance using the following recursions:

$$\begin{aligned}
\zeta_k &= \sigma_k - E(y_k|\mathcal{F}_{k-1})\\
E(\beta_k|\mathcal{F}_k) &= E(\beta_k|\mathcal{F}_{k-1}) + \mathcal{K}_k\zeta_k\\
\Sigma(\beta_k|\mathcal{F}_k) &= (\mathcal{I} - \mathcal{K}_k\mathbf{F})\Sigma(\beta_k|\mathcal{F}_{k-1})
\end{aligned} \tag{11}$$

where

$$\mathcal{K}_k = \Sigma(\beta_k|\mathcal{F}_{k-1})\mathbf{F}^T\Sigma(\sigma_k|\mathcal{F}_{k-1})^{-1} \tag{12}$$

The above steps are repeated for every time step to get the estimates of the prediction error (ζ_k) and the covariance matrix of the state vectors ($\Sigma(\beta_k|\mathcal{F}_{k-1})$). Under the assumption of Gaussian error terms, the log-likelihood function takes the following form:

$$l(\theta) = -\frac{1}{2}\sum_{k=1}^{N}\left(n_k \ln 2\pi + \ln(\det(\Sigma(\beta_k|\mathcal{F}_{k-1})) + \zeta_k^T\Sigma(\beta_k|\mathcal{F}_{k-1})^{-1}\zeta_k\right) \tag{13}$$

where N is the number of time points in the sample, and n_k is the number of observations at time point k.

The model specification and steps for estimation for the DQ model are exactly analogous.

$$\begin{aligned} y_t(\Delta) &= a_t\Delta^2 + b_t\Delta + c + \epsilon_t && \text{Measurement equation} \\ \beta_t &= \mathbf{C} + \mathbf{A}\beta_{t-1} + \eta_t && \text{State equation} \end{aligned} \tag{14}$$

where, in this case, $\beta_t \equiv \{a_t, b_t, c_t\}$.

5. Results

5.1. Preliminary analysis

For comparing the performance and parameter stability across models, it is useful to have a reference point. And the simplest, and arguably the most natural, reference point is the IV corresponding to $\Delta = 0$ (deep OTM options), which we refer to as IV_{OTM}. In the quadratic model, IV_{OTM} is captured by the coefficient c, and that in the NS model is captured by the sum of the first two coefficients, $\beta_0 + \beta_1$ (as $\Delta \to 0$; see Nelson and Siegel, 1987). To begin with, we use the IV_{OTM} estimate to compare the in-sample performance and the stability of factors estimates across the four models.

Figure 2 represents time series evolution of IV_{OTM} for the four methods for a sample stock (ticker RELIANCE). Except for the NS model, which shows large in-sample variation, the corresponding values from the other three models are comparable. Given the high variation in IV_{OTM} from the NS model (as seen in the top panel of figure 2), the bottom panel separately compares IV_{OTM} from DNS, DQ and SQ models. Although not shown here, we find the same pattern for all the stocks considered in the sample (results available on request).

[Insert Figure 2 about here]

Next, to quantify the stability of parameters, we use the standard deviation of the first difference of the estimates, and for comparing the in-sample fit we use the Root Weighted Mean Squared Error (RWMSE), as defined earlier in equation 6. Table 2 provides a summary of these measures (mean value across 100 symbols) across the four models. The top panel presents the result for the two NS variants, and the bottom panel presents the results of two quadratic models. For both types, the dynamic specification provides more stable factor estimates than their static counterparts. The difference is even more stark in the case of NS and DNS. The NS model has four free parameters (β_0, β_1, β_2, λ), as compared to three in the quadratic model (a, b, c). It is evident that this additional flexibility of the NS model comes at the cost of possible overfitting. The NS seems useful only in its dynamic avatar, the DNS model. On the other hand, for most of the stocks, SQ model provides better in-sample fit than its dynamic counterpart. However, the difference in the RWMSE across the four models is marginal (in the range of 0.1% to 0.3%) for most of the stocks.

[Insert Table 2 about here]

5.2. A trading strategy based on mis-pricing

While the in-sample fit is a good measure to assess the ability of a model to match the observed shape of the volatility smile, it is neither a necessary nor a sufficient condition for the model's success in a real world trading environment. A better measure of predictive ability for the task at hand is the trading profits or returns generated by a trading strategy based on the competing models.

Our preferred trading strategy follows the popular market-neutral long-short portfolio approach widely used in the empirical asset pricing literature (Jegadeesh and Titman, 1993; Pástor and Stambaugh, 2003; Fama and French, 1993). This formulation allows us to tease out the variation in the excess return contributed by the specific risk factors or anomalies after controlling for other risk factors. Goyal and Saretto (2009) use a similar approach in the context of option markets, where they explore the relationship between option returns and the difference between historical realized volatility and ATM IV. Although, in principle, we also explore the relationship between the pricing error (measured by the difference between market price and model price) and option returns after controlling for other risk factors for the options (as measured by option Greeks), our objective here is more aligned with the idea of statistical arbitrage. Our approach is based on earning almost riskless profit by buying the undervalued and selling the overvalued options implied by the model. The step-by-step details of the trading strategy as implemented by us is described below.

[Insert Table 3 about here]

Step 1. Identification of options to trade: Every day, we divide the traded options in 10 deciles based on their pricing error (market price−model price). Our preferred trading strategy buys the cheapest or most undervalued options (bottom 10% of options ranked by market price model price) and sells the most expensive or overvalued options (top 10% of options ranked by market price−model price). We also consider buying the bottom 20% (undervalued) options and selling the top 20% (overvalued options) and seven other strategies for selecting options to trade (these are listed in Table 3). However, these alternative strategies do not perform as well as our preferred strategy which is also intuitively understandable.

Step 2. Weighting of options: For simplicity and better diversification, we choose to equally weight all the options in the long side of the trade, and separately equally weight all the options in the short side of the trade.

Step 3. Scaling of the long versus short side of the trading portfolio: In order to reduce the risk of the strategy as much as possible, we scale the long and short portfolios to have equal (and opposite) vega so that the total trading portfolio is vega-neutral. We do not equate the market value of the options on the long and short side, because the capital required to support this trade has very little to do with the net option premium. As explained below, the economic capital required to support the trade is estimated using the margin rules of the derivatives exchange (in this case, the NSE clearing corporation). Also, we do not try to equate the notional value or the option

delta of the long and short side because we can (and do) use the liquid SSF market to make the portfolio delta-neutral. The only material choice here is between gamma and vega-neutrality, but gamma is more relevant in a hold-to-maturity paradigm, while (subject to liquidity considerations) we seek to trade out of our positions as soon as the market price converges to the model price.

Step 4. *Exit strategy*: As mentioned above, our preference is to trade out of our positions as soon as the market price converges to the model price. But this is not always possible because some strikes may be relatively illiquid to begin with. Moreover, even an option that was liquid at inception could become illiquid subsequently if the underlying moves significantly causing the strike to stray far from the money. If we are unable to exit the position due to illiquidity, we hold the option to maturity and calculate the payoff at expiry by using the SSF price. We rebalance the portfolio on a daily basis to maintain delta and vega-neutrality.

Step 5. *Economic capital and rate of return*: We calculate profit of every symbol for each expiry cycle independently, resulting in 1,200 profit observations (100 stocks $\times$ 12 expiry cycles). To calculate the rate of return, we divide the realized profit of the trading strategy by the economic capital required for the strategy. We estimate the economic capital using the SPAN methodology used by the NSE to determine portfolio margins. This capital requirement is also a close approximation to the regulatory capital, but it could be an underestimate because the exchange also levies certain other margins like intraday margins which we ignore for our study. The use of margin rules to estimate capital requirements and rate of return is well established in the literature (Murray, 2013).

Step 6. *Accounting for transaction costs*: Our objective of this analysis is twofold: first, to demonstrate that market price of the option contracts has a tendency to revert to the model price implied by the respective models. For this purpose, we use the last traded price as the execution price. However, this assumption might not be realistic from the trading perspective, because of the presence of bid-ask spread. In the next set of analysis, we explore whether the mispricing in the option market is significant enough for traders to earn profit, even after considering the impact of bid-ask spread. Here, we approximate the ask price (price at which trader can buy) by adding half of the average bid-ask spread for the day for that particular contract, and similarly for the bid price (price at which trader can sell), by subtracting half of the average bid-ask spread for the day for that particular contract. The bid-ask spread is determined by averaging the bid-ask spreads at five different time stamps during the day. NSE provides the five order book snapshots, taken at 11:00, 12:00, 13:00, 14:00 and 15:00 hours. We first compute the bid-ask spread for each option contract using the order book snapshots and then use the average of the bid-ask spreads as a measure of the transaction cost. Although tedious and demanding, this granular approach of calculating contract-wise bid-ask spread enables us to filter out extremely illiquid deep ITM and OTM strikes from our trading sample, which

are suspected to be used for tax manipulation purposes (Jain et al., 2019) with the possibility of trade happening at a very unreasonable price.

Step 7. Setting a placebo sample - a random portfolio: To ascertain that the trading profit is generated solely because of the mispricing captured by the model, and not by design of the trading strategy itself, we also create a placebo long-short portfolio. This strategy, referred to as random strategy henceforth, randomly selects 10% of the traded option contracts to buy and 10% of the traded option contracts to sell. The rest of the implementation follows the exact procedure of trading strategy described earlier.

This completes our description of the steps involved in implementing our trading strategy.

Table 4 provides a comparison of the performance of our preferred trading strategy of buying the top decile and selling the bottom decile across different estimation models. Panel A provides the performance summary of the trading strategy, where we assume that orders are executed on the last traded price without accounting for transaction costs, and panel B provides the performance summary of the trading strategy after accounting for the transaction costs on the order execution.

The 'win rate' row provides the percentage of positive return observations in the sample, and the next five rows provide the summary statistics of the return observation measured in percentage points. The last three rows respectively provide the Sharpe ratio, the 5th percentile and the mean of the profits in Indian Rupees (INR). As described earlier, we scale the long and short portfolios to have equal (and opposite) vega. Thus, the cash profit earned on any of the strategies is also a scaled measure (INR earned on 1000 vega long and short exposure), and therefore they can be compared across strategies. Note that the negative of the 5th percentile of the profit in INR is the associated 95% Value at Risk for the strategy.

[Insert Table 4 about here]

In the first set of results shown in panel A, all four models perform much better than the random strategy on all the performance criteria. As expected, the random strategy has around 50% win rate compared to the win rate of around 88-90% for the four models. Overall, the dynamic models outperform their static counterparts, with the DNS performing the best on most of the criteria (except on the Sharpe ratio, where DQ performs the best). In the second set of results, panel B summarises our main result relevant from a trading perspective. In this, we also consider additional transaction costs implied by bid-ask spread. While, as expected, the overall performance of the second trading strategy across models is significantly inferior, now the superiority of dynamic models comes across as even more pronounced, suggesting that the performance of the static models might be inflated in the earlier case because of the inclusion of less liquid contracts in the trading sample. The DNS model now outperforms all other models with a 65% win rate and 104% annualized average return, followed by the DQ model.

[Insert Table 5 about here]

We also examine the statistical significance of the difference in the trading returns between dynamic and static models. As the paired differences of the trading returns do not have a Normal distribution, we conduct a one-sided paired Wilcoxon Rank test on the paired observations of selected models' trading returns. Table 5 provides p-value of the paired Wilcoxon Rank test, with the alternative hypothesis that the returns generated by model in row-names are greater than the returns generated by model in the column-name. As earlier, panel A presents the results without considering the impact of transaction costs, while panel B does so. The results confirm the superiority of DNS model over all other models with a p-value of < 0.01 in all cases but one. When transaction costs are considered, the DQ model provides statistically significant higher returns than its static counterpart.

As a robustness check, we also consider eight additional trading strategies depending on the decile buckets considered for buying and selling securities. Table 3 provides brief description of these strategies, and figures 3 and 4 provide boxplots for trading returns generated by these strategies both with and without bid-ask spreads. As expected, the performance of the trading strategies deteriorate as the option selection criteria approach the median decile. But as earlier, here also the DNS model outperforms other models for most of the strategies even if the majority of strategies generate a negative median return after accounting for transaction costs. Overall, our results show that the trading returns generated by the preferred '10-1' strategy using the DNS model are neither driven by any particular industry, nor by any specific period. The trend of superiority of the DNS model remains even with trading strategies based on other deciles.

[Insert Figure 3 about here]

[Insert Figure 4 about here]

5.3. Determinants of profit from the trading strategy

Finally, we demonstrate that trading return is not driven by portfolio exposure to other systematic risk factors relevant to options markets. Given that our portfolio is designed to be both delta and vega-neutral, we regress portfolio return on other option Greeks, including theta, rho, gamma, vanna and vomma. As is well known in the option pricing literature, theta measures the sensitivity of an option's price with respect to time to maturity, rho measures the sensitivity of the option's price with respect to risk-free interest rate, and the higher order Greeks, gamma, vomma and vanna respectively capture option convexity to stock price and volatility, and sensitivity of vega to delta. For each underlying stock, we calculate these Greeks on a daily basis and then average them over the expiry cycle. Using a random effects panel data approach, we then regress the trading returns against the Greeks while controling for size (measured as log of market capitalization) and industry and expiration-date fixed effects. Table 7 summarises the regression results. Our main result is presented in the first column, where we account for transaction costs, i.e. returns are adjusted for the effect of bid-ask spread. The results in column 2 do not consider the transaction costs.

[Insert Table 7 about here]

We find that none of the option Greeks have significant explanatory power for the portfolio returns, indicating that the trading returns are primarily driven by the mispricing captured by the DNS model. A negative and statistically significant coefficient for log(market capitalization) without accounting for bid-ask spread suggests that less profitable mispricing is in options written on large stocks than in small stocks. This is not surprising, given that the pricing of options on large stocks tends to be more efficient. Also, the higher transaction costs for trading options on small stocks would likely have a negatively influence on the trading returns. The results in column 2 only captures the first channel, while results in column 1 likely capture both the impacts simultaneously. It appears that mispricing in small-sized stocks is partially offset by the higher transaction costs required to execute trades in these stocks. While the coefficients are still negative, they are not statistically significant. We observe a similar pattern of diminishing influence in the COVID-19 month (the March 2020 expiration cycle), a period of high uncertainty. Here also we observe positive and statistically significant fixed effects in the March 2020 expiration cycle in column 1 results. And in line with the rest of the results, when we do not consider transaction costs, the effect is much higher. As demonstrated in table 1, there is also evidence of a wider bid-ask spread in March, 2020, which should negatively influence the coefficients. However, in this case, the coefficient is still significant. We also have negative and positive fixed effects in August and September. Although not reported here, we do not find any statistically significant evidence for industry-fixed effects.

As our sample period coincides with the COVID-19 pandemic, we also try and understand if COVID-19 induced uncertainty (Agarwalla et al., 2021a) impacts the trading results. Figure 5 displays the time series plot of the benchmark stock index – NIFTY (blue line) and the India VIX (green line) for the sample period. Although the pandemic was not yet over when our sample period ends, the financial market witnessed the greatest uncertainty in March 2020, with large stock market declines and the India VIX levels exceeding 80%. To analyze the impact of COVID-19, following Agarwalla et al. (2021b), we divide our sample into three sub-periods: pre-COVID (January-February, 2020), COVID (March, 2020), and post-COVID (April to December, 2020).

[Insert Figure 5 about here]

Table 6 presents the summarized trading returns across industry and the three subperiods. The increased market uncertainty can impact trading profits in both directions. Because of uncertainty and forced liquidation due to funding constraints, option prices can deviate further from their fair values. However, these mispricings may not necessarily result in a trading profit, as they may not revert to zero because of limits to arbitrage (Shleifer and Vishny, 1997). As the stock market witnessed some signs of recovery in late March, we should also anticipate some reversion of the fear-induced mispricing. For certain industries, such as Consumer Discretionary, Energy Finance, Healthcare, Industrials, Materials, Real Estate and Utilities, the COVID month has a much higher return than the pre-COVID and

post-COVID period. However, industries such as Communication, Consumer Goods and Software generate lower and even negative mean returns during the COVID period.

[Insert Table 6 about here]

6. Conclusion

The language of options markets is that of IV, and in addition ascertaining options market's view of future returns and for pricing exotic derivatives, an economically meaningful and flexible model for implied volatility is also essential for implementing option trading strategies.

Drawing on the analogy of a volatility smile as interest rate term structure, we have used the DNS approach popular in the fixed income markets to model the dynamics of volatility smile with respect to option delta. While it has been used in the literature earlier to capture the term structure of volatility smile, to our knowledge, ours is the first study which has used it to model the dynamics of the smile with respect to delta and evaluated its performance in a trading environment while accounting for transaction costs.

Using stock options data from NSE, one of the few markets worldwide with a liquid stock options market along with a simultaneously liquid stock futures market (and so allowing for a clean computation of implied volatility), we show that the DNS model consistently outperforms all other competing specifications on most of our selected criteria. Our trading strategy is based on rank ordering the options based on mispricing, and going long the options in the upper deciles and going short the options in the lower decile. Our 10-1 strategy performs the best (long the last decile and short the first decile), but our results are robust to other trading strategies which follow the same logic as our preferred strategy.

We find that none of the option Greeks have significant explanatory power for the portfolio returns, indicating that the trading returns are primarily driven by the mispricing captured by the Dynamic Nelson Siegel model. We also tried to assess if COVID-19 induced uncertainty impacts our trading results, and we find that for certain industries, such as Consumer Discretionary, Energy Finance, Healthcare, Industrials, Materials, Real Estate and Utilities, the COVID month has a much higher return than the pre-COVID and post-COVID period. However, industries such as Communication, Consumer Goods and Software generate lower and even negative mean returns during the COVID period.

Beyond showing the success of the specific DNS model, we argue that for modeling volatility smile for trading purposes, dynamic models outperform their static counterparts, with the worst dynamic model outperforming the best static model in terms of the win rate (percentage of positive returns in the sample). Further, we show that when it comes to static models, the more parsimonious quadratic models do distinctly better, but when it comes to a dynamic setting, the DNS model is significantly superior to the Dynamic Quadratic model. The lesson here is that a more flexible model needs more data to be effective.

References

Agarwalla, S.K., Varma, J.R., Virmani, V.. The impact of COVID-19 on tail risk: Evidence from nifty index options. Economics Letters 2021a;204:109878. doi:https://doi.org/10.1016/j.econlet.2021.109878.

Agarwalla, S.K., Varma, J.R., Virmani, V.. Rational repricing of risk during covid-19: Evidence from indian single stock options market. Journal of Futures Markets 2021b;41(10):1498–1519. doi:https://doi.org/10.1002/fut.22240.

Alexander, C.. Principal component analysis of volatility smiles and skews. Available at SSRN 248128 2001;.

Bedendo, M., Hodges, S.D.. The dynamics of the volatility skew: A kalman filter approach. Journal of Banking & Finance 2009;33(6):1156–1165. doi:https://doi.org/10.1016/j.jbankfin.2008.12.014.

Black, F.. The pricing of commodity contracts. Journal of financial economics 1976;3(1-2):167–179.

Black, F., Scholes, M.. The pricing of options and corporate liabilities. Journal of Political Economy 1973;81(3):637–654.

Bollen, N.P.B., Whaley, R.E.. Do expirations of hang seng index derivatives affect stock market volatility? Pacific-Basin Finance Journal 1999;7:453–470.

Bollen, N.P.B., Whaley, R.E.. Does net buying pressure affect the shape of implied volatility functions? The Journal of Finance 2004;59(2):711–753. doi:https://doi.org/10.1111/j.1540-6261.2004.00647.x.

Carr, P., Wu, L.. What type of process underlies options? a simple robust test. The Journal of Finance 2003;58(6):2581–2610. doi:https://doi.org/10.1046/j.1540-6261.2003.00616.x.

Chalamandaris, G., Tsekrekos, A.E.. How important is the term structure in implied volatility surface modeling? evidence from foreign exchange options. Journal of International Money and Finance 2011;30(4):623–640. doi:https://doi.org/10.1016/j.jimonfin.2011.02.001.

Chalamandaris, G., Tsekrekos, A.E.. Predictability in implied volatility surfaces: evidence from the euro otc fx market. The European Journal of Finance 2014;20(1):33–58. doi:10.1080/1351847X.2012.670123.

Chen, Y., Han, Q., Niu, L.. Forecasting the term structure of option implied volatility: The power of an adaptive method. Journal of Empirical Finance 2018;49:157–177. doi:https://doi.org/10.1016/j.jempfin.2018.09.006.

Chen, Y., Niu, L.. Adaptive dynamic nelsonsiegel term structure model with applications. Journal of Econometrics 2014;180(1):98–115. doi:https://doi.org/10.1016/j.jeconom.2014.02.009.

Choi, Y., Jordan, S.J., Lee, W.. Information content in sneer asymmetry: An application to out-of-sample implied volatility forecasting. Emerging Markets Finance and Trade 2015;51(sup3):34–51. doi:10.1080/1540496X.2015.1039900.

Christoffersen, P., Heston, S., Jacobs, K.. The shape and term structure of the index option smirk: Why multifactor stochastic volatility models work so well. Management Science 2009;55(12):1914–1932.

Cont, R., Fonseca, J.d.. Dynamics of implied volatility surfaces. Quantitative Finance 2002;2(1):45–60. doi:10.1088/1469-7688/2/1/304.

Cortazar, G., Schwartz, E.S., Naranjo, L.F.. Term-structure estimation in markets with infrequent trading. International Journal of Finance & Economics 2007;12:353–369. doi:10.1002/ijfe.317.

Dennis, P., Mayhew, S.. Risk-neutral skewness: Evidence from stock options. The Journal of Financial and Quantitative Analysis 2002;37(3):471–493.

Derman, E., Kamal, M., Kani, I., McClure, J., Pirasteh, C., Zou, J.. Investing in Volatility. Quantitative Strategies Research Notes 3514894; Goldman Sachs; 1996.

Derman, E., Kani, I.. Riding on a smile. Risk 1994;7(2):32–39.

Derman, E., Miller, M.B.. The volatility smile. John Wiley & Sons, 2016.

Diebold, F.X., Li, C.. Forecasting the term structure of government bond yields. Journal of Econometrics 2006;130:337–364. doi:10.1016/j.jeconom.2005.03.005.

Dumas, B., Fleming, J., Whaley, R.E.. Implied volatility functions: Empirical tests. The Journal of Finance 1998;53(6):2059–2106. doi:https://doi.org/10.1111/0022-1082.00083.

Dupire, B.. Pricing with a smile. Risk 1994;7(1):18–20.

Fama, E.F., French, K.R.. Common risk factors in the returns on stocks and bonds. Journal of financial economics 1993;33(1):3–56.

Fengler, M.R., Hin, L.Y.. Semi-nonparametric estimation of the call-option price surface under strike and time-to-expiry no-arbitrage constraints. Journal of Econometrics 2015;184(2):242–261. doi:https://doi.org/10.1016/j.jeconom.2014.09.003.

Foresi, S., Wu, L.. Crash–o–phobia. The Journal of Derivatives 2005;13(2):8–21. doi:10.3905/jod.2005.605352.

Franke, G., Stapleton, R.C., Subrahmanyam, M.G.. Who buys and who sells options: The role of options in an economy with background risk. Journal of Economic Theory 1998;82(1):89–109. doi:https://doi.org/10.1006/jeth.1998.2420.

Franois, P., Stentoft, L.. Smile-implied hedging with volatility risk. Journal of Futures Markets 2021a;41(8):1220–1240. doi:https://doi.org/10.1002/fut.22191.

Franois, P., Stentoft, L.. Smile-implied hedging with volatility risk. Journal of Futures Markets 2021b;41(8):1220–1240. doi:https://doi.org/10.1002/fut.22191.

Garca-Machado, J.J., Rybczyski, J.. How spanish options market smiles in summer: an empirical analysis for options on ibex-35. The European Journal of Finance 2017;23(2):153–169. doi:10.1080/1351847X.2015.1067634.

Gatheral, J., Jusselin, P., Jusselin, P., Rosenbaum, M.. The Quadratic Rough Heston Model and the Joint S&P 500/VIX Smile Calibration Problem. SSRN Working Paper 3514894; SSRN Woking Paper; 2020.

Goyal, A., Saretto, A.. Cross-section of option returns and volatility. Journal of Financial Economics 2009;94(2):310–326.

Grnborg, N.S., Lunde, A.. Analyzing oil futures with a dynamic nelson-siegel model. Journal of Futures Markets 2016;36(2):153–173. doi:https://doi.org/10.1002/fut.21713.

Guidolin, M., Timmermann, A.. Option prices under bayesian learning: implied volatility dynamics and predictive densities. Journal of Economic Dynamics and Control 2003;27(5):717–769. doi:https://doi.org/10.1016/S0165-1889(01)00069-0.

Guo, B., Han, Q., Lin, H.. Are there gains from using information over the surface of implied volatilities? Journal of Futures Markets 2018;38(6):645–672. doi:https://doi.org/10.1002/fut.21903.

Guo, B., Han, Q., Zhao, B.. The nelsonsiegel model of the term structure of option implied volatility and volatility components. Journal of Futures Markets 2014;34(8):788–806. doi:https://doi.org/10.1002/fut.21653.

Hagan, P.S., Kumar, D., Lesniewski, A.S., Woodward, D.E.. Managing smile risk. Wilmott 2002;:84–108doi:10.1088/1469-7688/2/1/304.

Hayashi, F.. Analytically deriving risk-neutral densities from volatility smiles in delta. The Journal of Derivatives 2020;27(4):6–12.

Heston, S.L.. A Closed-Form Solution for Options with Stochastic Volatility with Applications to Bond and Currency Options. The Review of Financial Studies 1993;6(2):327–343. doi:10.1093/rfs/6.2.327.

Hull, J., White, A.. The pricing of options on assets with stochastic volatilities. The Journal of Finance 1987;42(2):281–300. doi:https://doi.org/10.1111/j.1540-6261.1987.tb02568.x.

Jackwerth, J.C.. Option-Implied Risk-Neutral Distributions and Risk Aversion. SSRN Working Paper 1303779; CFA Institute Research Foundation of AIMR Publications; 2004.

Jain, S., Varma, J.R., Agarwalla, S.K.. Indian equity options: Smile, risk premiums, and efficiency. Journal of Futures Markets 2019;39(2):150–163.

Jegadeesh, N., Titman, S.. Returns to buying winners and selling losers: Implications for stock market efficiency. The Journal of Finance 1993;48(1):65–91. URL: https://onlinelibrary.wiley.com/doi/abs/10.1111/j.1540-6261.1993.tb04702.x. doi:https://doi.org/10.1111/j.1540-6261.1993.tb04702.x. arXiv:https://onlinelibrary.wiley.com/doi/pdf/10.1111/j.1540-6261.1993.tb04702.x.

Jin, W., Livnat, J., Zhang, Y.. Option prices leading equity prices: Do option traders have an information advantage? Journal of Accounting Research 2012;50(2):401–432. doi:https://doi.org/10.1111/j.1475-679X.2012.00439.x.

Kearney, F., Shang, H.L., Sheenan, L.. Implied volatility surface predictability: The case of commodity

markets. Journal of Banking & Finance 2019;108:105657. doi:https://doi.org/10.1016/j.jbankfin.2019.105657.
Kim, B., Kim, D.H., Park, H.. Informed options trading on the implied volatility surface: A cross-sectional approach. Journal of Futures Markets 2020;40(5):776–803. doi:https://doi.org/10.1002/fut.22070.
Kim, S.. Portfolio of volatility smiles versus volatility surface: Implications for pricing and hedging options. Journal of Futures Markets 2021;41(7):1154–1176. doi:https://doi.org/10.1002/fut.22213.
Koopman, S.J., Jungbacker, B., Hol, E.. Forecasting daily variability of the S&P 100 stock index using historical, realised and implied volatility measurements. Journal of Empirical Finance 2005;12(3):445–475. doi:https://doi.org/10.1016/j.jempfin.2004.04.009.
Kou, S.G., Wang, H.. Option pricing under a double exponential jump diffusion model. Management Science 2004;50(9):1178–1192. doi:10.1287/mnsc.1030.0163.
Kumar, S., Virmani, V.. Term structure estimation with liquidity-adjusted affine nelson siegel model: A nonlinear state space approach applied to the indian bond market. Applied Economics 2022;54(6):648–669. doi:10.1080/00036846.2021.1967866.
Le, V., Zurbruegg, R.. Forecasting option smile dynamics. International Review of Financial Analysis 2014;35:32–45. doi:https://doi.org/10.1016/j.irfa.2014.07.006.
Liu, D., Liang, Y., Zhang, L., Lung, P., Ullah, R.. Implied volatility forecast and option trading strategy. International Review of Economics & Finance 2021;71:943–954. doi:https://doi.org/10.1016/j.iref.2020.10.023.
Malz, A.M.. Estimating the probability distribution of the future exchange rate from option prices. Journal of Derivatives 1997;5(2):18–36.
Merton, R.C.. Theory of rational option pricing. The Bell Journal of Economics and Management Science 1973;4(1):141–183.
Mixon, S.. Option markets and implied volatility: Past versus present. Journal of Financial Economics 2009;94(2):171–191.
Murray, S.. A margin requirement based return calculation for portfolios of short option positions. Managerial Finance 2013;.
Nagy, K.. Term structure estimation with missing data: application for emerging markets. The Quarterly Review of Economics and Finance 2020;75:347–360.
Nelson, C.R., Siegel, A.F.. Parsimonious modeling of yield curves. The Journal of Business 1987;60:473. doi:10.1086/296409.
Park, H., Kim, B., Shim, H.. A smiling bear in the equity options market and the cross-section of stock returns. Journal of Futures Markets 2019;39(11):1360–1382. doi:https://doi.org/10.1002/fut.22000.
Pástor, L., Stambaugh, R.F.. Liquidity risk and expected stock returns. Journal of Political economy 2003;111(3):642–685.
Rebonato, R.. Volatility and Correlation: The Perfect Hedger and the Fox. 2nd ed. Wiley, 2004.
Rebonato, R., McKay, K., White, R.. The SABR/LIBOR Market Model: Pricing, Calibration and Hedging for Complex Interest-Rate Derivatives. 1st ed. Wiley, 2009.
Reiswich, D., Wystup, U.. Fx volatility smile construction. 2009.
Rogers, L.C.G., Tehranchi, M.R.. Can the implied volatility surface move by parallel shifts? Finance and Stochastics 2010;14(2):235–248. doi:10.1007/s00780-008-0081-9.
Rubinstein, M.. Implied binomial trees. The Journal of Finance 1994;49(3):771–818.
Shleifer, A., Vishny, R.W.. The limits of arbitrage. The Journal of finance 1997;52(1):35–55.
Stein, E.M., Stein, J.C.. Stock Price Distributions with Stochastic Volatility: An Analytic Approach. The Review of Financial Studies 1991;4(4):727–752. URL: https://doi.org/10.1093/rfs/4.4.727. doi:10.1093/rfs/4.4.727. arXiv:https://academic.oup.com/rfs/article-pdf/4/4/727/24417268/040727.pdf.
Sui, C., Lung, P., Yang, M.. Predictable dynamics in the implied volatility surface based on weighted least squares: Evidence from soybean meal futures options in china. Emerging Markets Finance and Trade 2020;56(11):2625–2638. doi:10.1080/1540496X.2019.1616543.
Taylor, S.J., Yadav, P.K., Zhang, Y.. The information content of implied volatilities and model-free

volatility expectations: Evidence from options written on individual stocks. Journal of Banking & Finance 2010;34(4):871–881. doi:https://doi.org/10.1016/j.jbankfin.2009.09.015.

Vogt, E.. Option-Implied Term Structures. Staff Reports 706; Federal Reserve Bank of New York; 2016.

Wong, A.H.S., Heaney, R.A.. Volatility smile and one-month foreign currency volatility forecasts. Journal of Futures Markets 2017;37(3):286–312. doi:https://doi.org/10.1002/fut.21799.

World Federation of Exchanges, . WFE/IOMA Derivatives Market Survey 2020. World Federation of Exchanges 2021;.

Yue, T., Gehricke, S.A., Zhang, J.E., Pan, Z.. The implied volatility smirk in the chinese equity options market. Pacific-Basin Finance Journal 2021;69:101624. doi:https://doi.org/10.1016/j.pacfin.2021.101624.

Zhang, J.E., Xiang, Y.. The implied volatility smirk. Quantitative Finance 2008;8(3):263–284. doi:10.1080/14697680601173444.

7. Figures

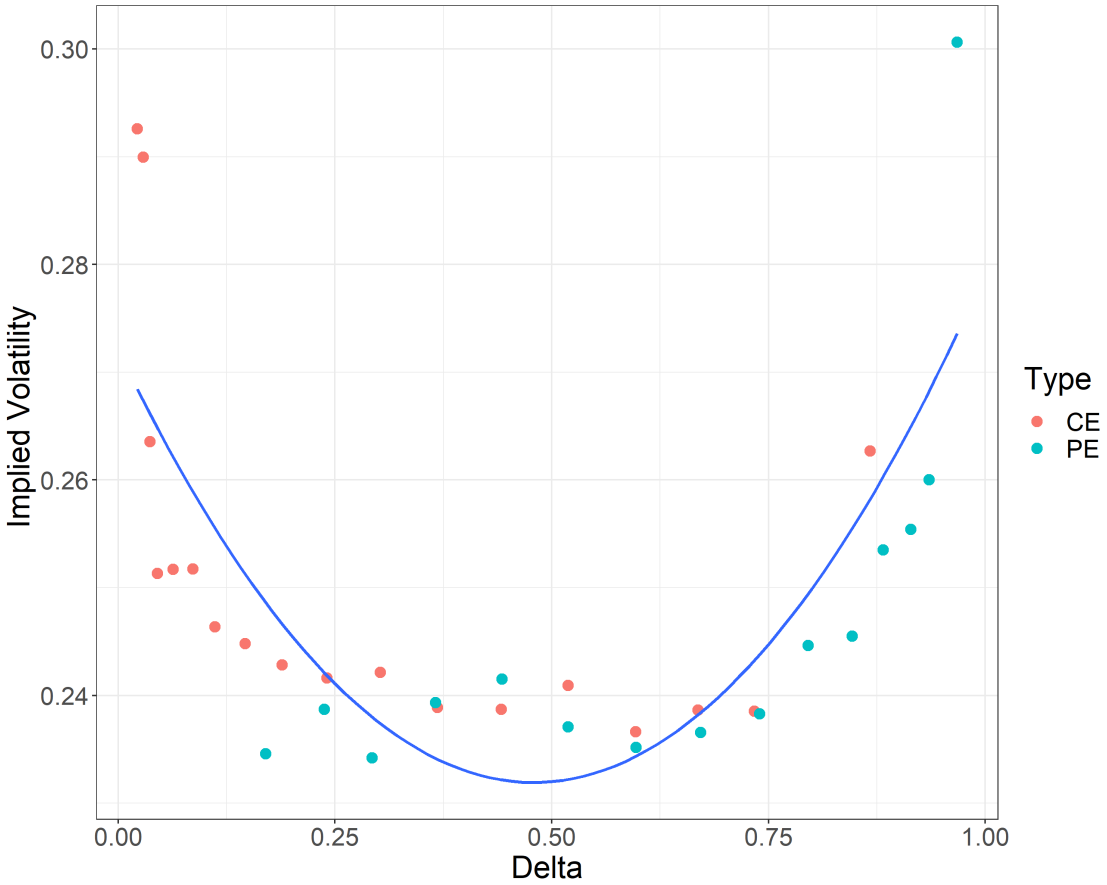

Figure 1: An example volatility smile. This figure shows the observed volatility smile for an example stock (ticker RELIANCE) as on January 1, 2020. The x-axis represents the option Δ and the y-axis represents the implied volatility.

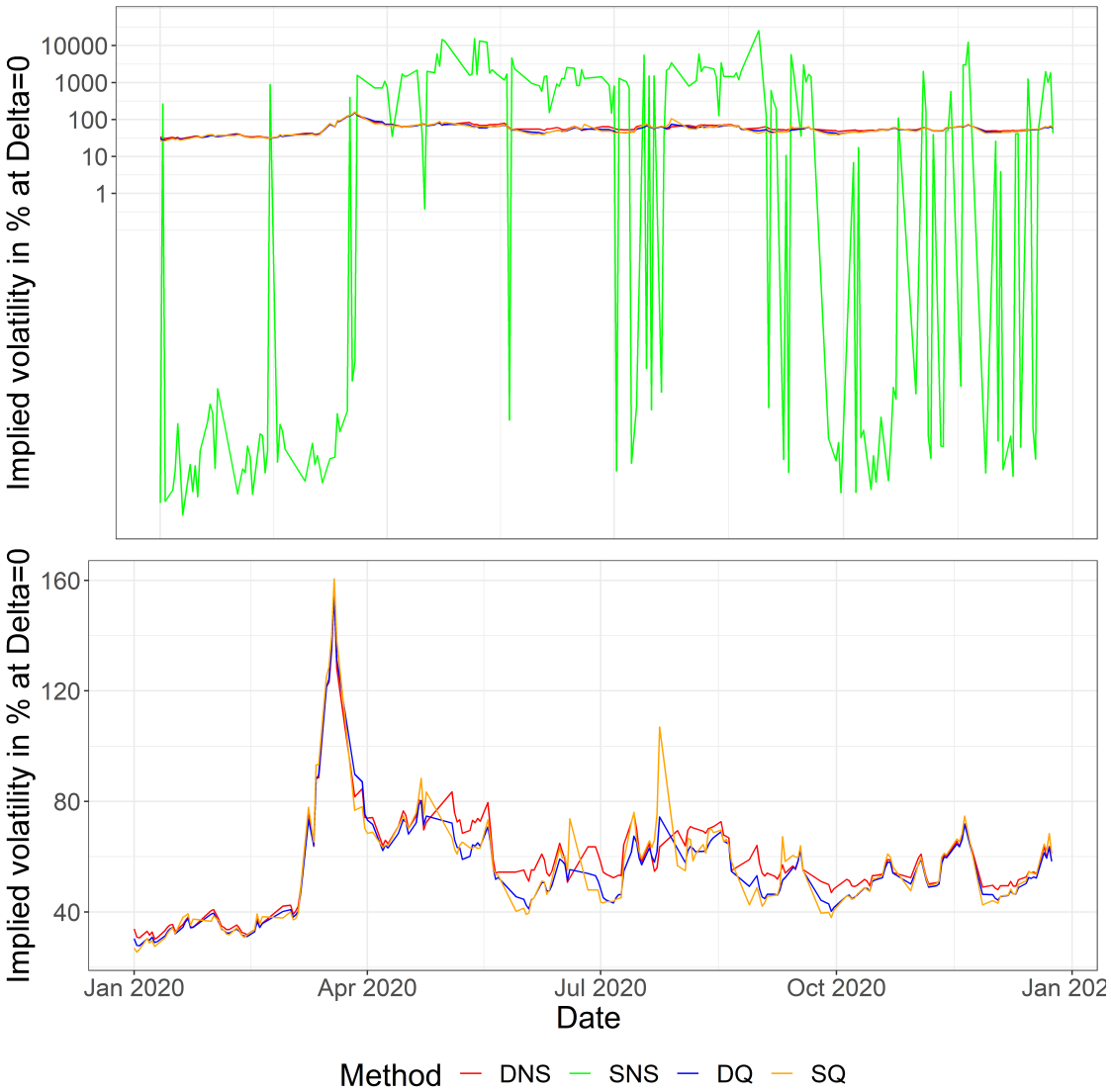

Figure 2: Comparison of model estimates of IV_{OTM}. The top panel of the figure compares the estimate of IV_{OTM} from the four models (DNS, NS, DQ and SQ) in a semi-log plot for an example stock (ticker RELIANCE). Given the high variation in IV_{OTM} from the NS model, the bottom panel separately compares IV_{OTM} from DNS, DQ and SQ models.

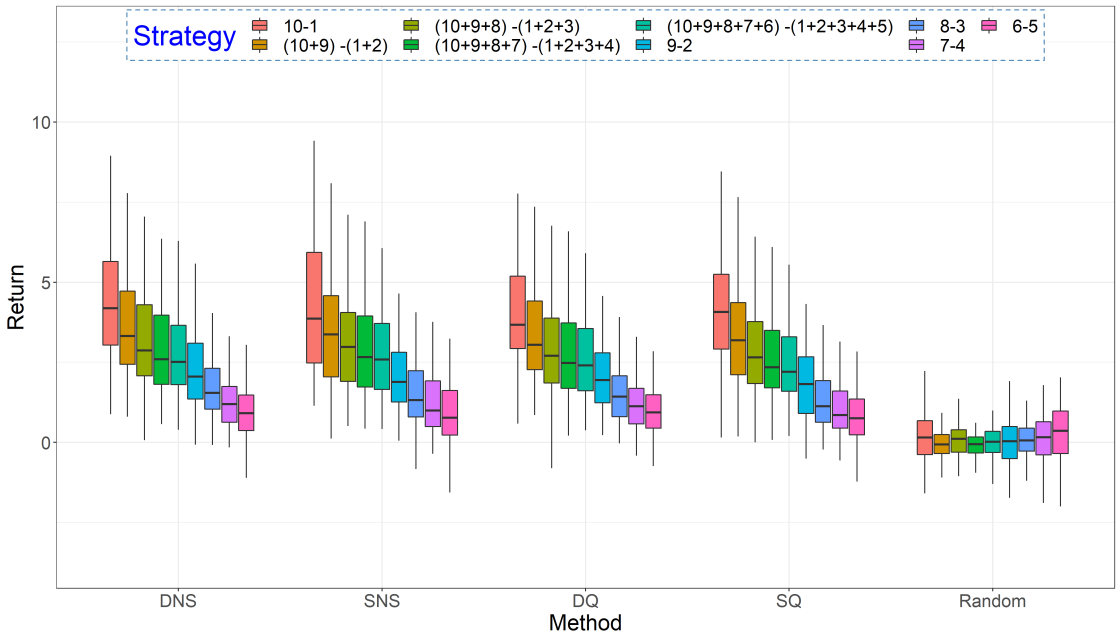

Figure 3: Returns from different trading strategies without accounting for the transaction cost. This figure provides the box plots of the returns generated on different trading strategies for all the four estimation models. The returns are represented as a number, for example, where 1 implies 100%. The transaction price is taken to be the last traded price without considering the impact of bid-ask spread.

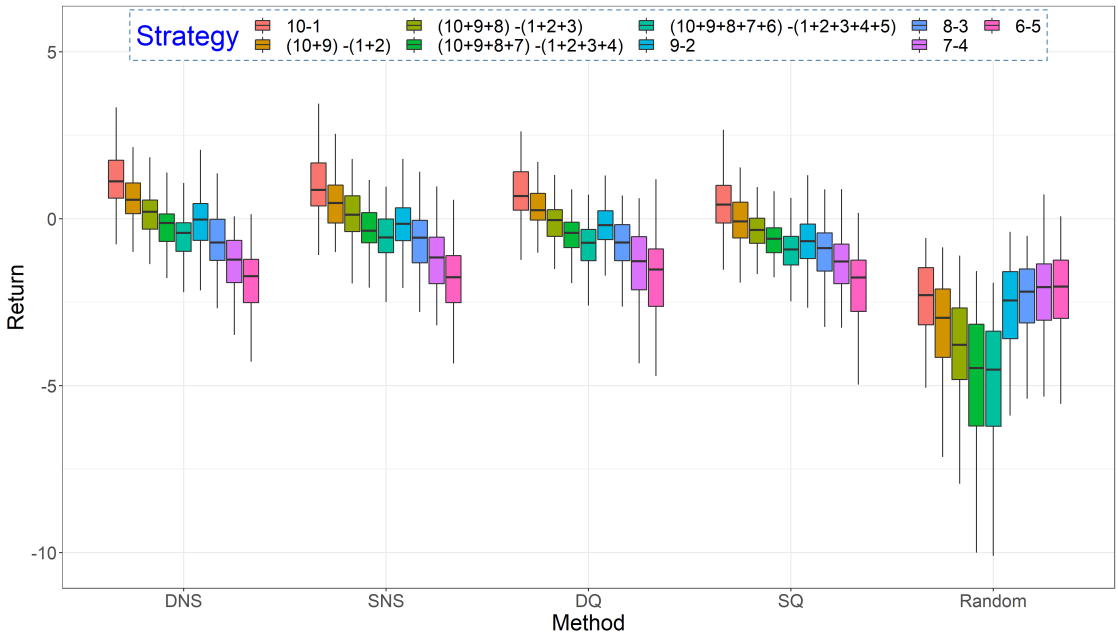

Figure 4: Returns on different trading strategies after accounting for transaction costs. The figure provides the box plots of the returns (represented in number, where 1 implies 100%) generated on different trading strategies for all the four estimation models. Here, the transaction price is taken to be the last traded price net of half the average bid-ask spread.

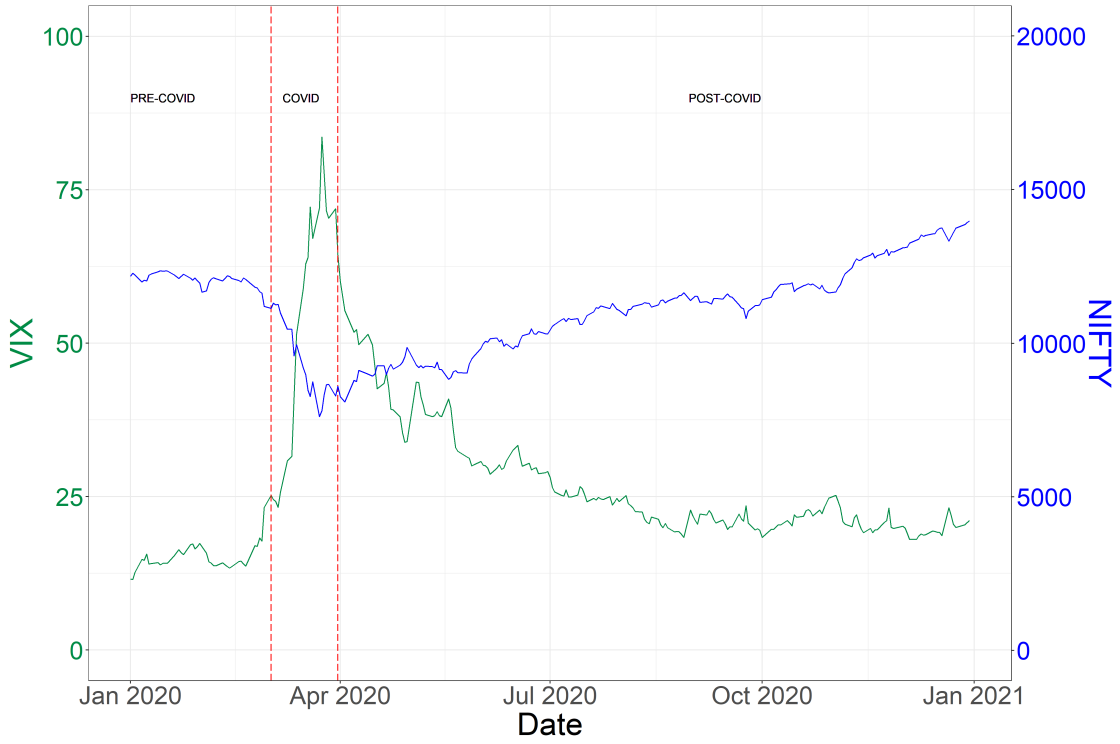

Figure 5: Impact of COVID-19. This figure describes the impact of the COVID-19 pandemic for Nifty returns and the India VIX. The blue line represents the time series plot of Indian benchmark index (Nifty) for the year 2000 (axis represented on the right side), while the green line represents the time series plot of the India VIX published by NSE. The sample is divided into three sub-periods to analyze the impact of COVID-19: Pre-COVID (January 2020 to February 2020), COVID (March, 2020), and Post-COVID (April 2020 to December 2020). See the main text for further discussion.

Tables

Table 1: Summary statistics. This table provides the summary of the observations across delta for call (left panel) and put (right panel) options. The delta of put option is converted into delta of the corresponding call option to make the range of Delta in (0, 1]. Panel A provides the summary of the full sample, while panel B provides the summary of the subsample of March 2020 (high volatility post COVID). Column 'N' presents the monthly average of number of observations, 'Bid-ask Spread (%)' presents the average bid-ask spread divided by option price in percentage terms, 'Volume' presents the average monthly traded volume, and 'N(trades)' presents the average monthly number of trades.

A: Full Sample

	Call Option				**Put Option**			
Delta	N	Bid-ask Spread (%)	Volume (in 10^9)	N (trades) (in 1000)	N	Bid-ask Spread(%)	Volume (in 10^9)	N (trades) (in 1000)
(0,0.1]	4,544.17	0.28	1.24	528.71	290.83	0.07	0.02	6.24
(0.1,0.2]	3,803.58	0.12	2.71	1,279.95	507.08	0.06	0.04	15.87
(0.2,0.3]	2,960.83	0.07	3.29	1,593.84	743.83	0.06	0.09	43.70
(0.3,0.4]	2,557.92	0.04	3.60	1,862.88	1,212.25	0.05	0.26	136.76
(0.4,0.5]	2,346.17	0.04	3.81	2,011.36	1,862.42	0.05	0.76	428.58
(0.5,0.6]	2,122.17	0.04	2.61	1,365.76	2,160.75	0.04	1.55	892.58
(0.6,0.7]	1,675.92	0.05	1.12	537.00	2,283.58	0.04	1.82	1,024.53
(0.7,0.8]	1,267.33	0.05	0.40	189.06	2,527.58	0.06	1.78	956.40
(0.8,0.9]	970.67	0.05	0.16	70.45	3,052.33	0.12	1.63	843.52
(0.9,1]	567.25	0.04	0.05	21.52	4,351.42	0.32	0.95	459.66

B: Subsample: March 2020

	Call Option				**Put Option**			
Delta	N	bid-ask Spread(%)	Volume (in 10^9)	N (trades) (in 1000)	N	Bid-ask Spread (%)	Volume (in 10^9)	N (trades) (in 1000)
(0,0.1]	7,728	0.36	1.81	647.97	1,725	0.09	0.09	39.45
(0.1,0.2]	3,854	0.20	2.44	1,058.34	1,735	0.10	0.12	54.78
(0.2,0.3]	2,553	0.13	2.38	1,143.07	1,522	0.09	0.17	86.17
(0.3,0.4]	2,054	0.10	2.11	1,084.18	1,558	0.09	0.37	194.76
(0.4,0.5]	1,798	0.12	1.67	889.69	1,698	0.09	0.89	464.15
(0.5,0.6]	1,425	0.13	0.87	466.50	1,745	0.09	1.42	751.18
(0.6,0.7]	835	0.13	0.28	137.64	1,766	0.10	1.45	722.28
(0.7,0.8]	371	0.11	0.07	40.96	1,843	0.13	1.32	615.94
(0.8,0.9]	90	0.13	0.01	4.06	1,731	0.20	0.87	360.63
(0.9,1]	10	0.18	0.0003	0.10	801	0.51	0.19	73.18

Table 2: In-sample fit versus the stability of the parameters. This table provides model-wise comparison of the stability of the parameter estimates as measured by the standard deviation (SD) of the first difference of the parameter, and in-sample fit as measured by the squared root of weighted mean squared error. The top panel presents the results for the two Nelson Siegel models, and the bottom panel presents the results for the two quadratic models.

		Nelson Siegel		
	SD(β_0)	SD(β_1)	SD(β_2)	RWMSE
Dynamic	0.13	0.11	0.27	0.0553
Static	17.95	42.82	322.58	0.0563
		Quadratic		
	SD(a)	SD(b)	SD(c)	RWMSE
Dynamic	0.13	0.13	0.06	0.0525
Static	0.49	0.41	0.1	0.0502

Table 3: Description of trading strategies. This table describes the nine trading strategies used in this study: Every day we rank the option contracts for a particular stock into 10 deciles based on their pricing error using the difference between the market price and the model price. For each strategy, the column 'Buy Decile' describes the decile buckets in which long positions are entered into, and the 'Sell Decile' column describes the decile buckets used for taking a short position in the options.

Strategy	Buy Decile	Sell Decile
1	1	10
2	1 + 2	10 + 9
3	1 + 2 + 3	10 + 9 + 8
4	1 + 2 + 3 + 4	10 + 9 + 8 + 7
5	1 + 2 + 3 + 4 + 5	10 + 9 + 8 + 7 + 6
6	2	9
7	3	8
8	4	7
9	5	6

Table 4: Performance of the preferred (10-1) trading strategy. The table provides a comparison of the performance of our preferred trading strategy - going long the 10th decile and short the first decile - across different estimation models. Under this strategy, every day the option contracts for a particular stock are ranked into 10 deciles based on their pricing error (market price − model price), and long position is taken in the undervalued bottom decile options and a short position in the overvalued top decile options. As a control, a random strategy is also used, where we 10% each of the total traded options are randomly selected to buy and sell. This strategy is run for every stock and for every expiry cycle independently, giving a total of 1200 profit observations (100 stocks × 12 expiry cycles). Panel A provides the performance summary of the trading strategy, without considering transaction costs (the bid-ask spreads), and panel B after considering accounting for the bid-ask spreads. It is assumed that buy/sell orders are executed on the approximate ask/bid price calculated by adding/subtracting the half the average bid-ask spread to the last traded price. The returns are calculated by dividing the trading profit with the average margin required to execute the trade. The 'win rate'row provides the percentage of positive return observations in the sample. The next five rows provide the summary statistics of the return observation measured in percentage points, and the final three rows provide the Sharpe ratio, the 5th percentile of the profit in INR, and the mean profit in INR.

A: Performance of the trading strategy (without transaction costs)					
	DNS	NS	DQ	SQ	Random
N	1200	1200	1200	1200	1200
Win rate	0.903	0.883	0.893	0.868	0.519
1st Quartile (Return)	127.493	80.702	124.442	121.683	-93.87
Median (Return)	312.140	269.143	287.830	329.166	7.549
Mean (Return)	437.965	386.640	406.660	430.130	-2.249
3rd Quartile (Return)	609.113	589.294	531.196	567.231	124.773
Std. Dev (Return)	652.158	1244.018	515.333	585.173	1259.82
Sharpe Ratio	0.666	0.308	0.782	0.729	-0.0048
5 Pct (Profit)	-255.123	-317.994	-297.945	-392.447	-1044.87
Mean (Profit)	1352.853	1255.216	1244.968	1076.794	-44.392
B: Performance of the trading strategy (with transaction costs)					
	DNS	NS	DQ	SQ	Random
Win rate	0.651	0.580	0.623	0.593	0.14
1st Quartile (Return)	-50.073	-65.834	-51.481	-90.1699	-351.549
Median (Return)	78.7842	34.858	50.421	46.76	-175.263
Mean (Return)	104.8072	70.78	74.865	33.308	-243.497
3rd Quartile (Return)	250.695	222.00	184.7005	186.4736	-60.829
Std. Dev.	775.1864	1227.77	559.609	616.324	572.5997
Sharpe Ratio	0.1304	0.054	0.127	0.0479	-0.432
5 Pct (Profit)	-981.551	-1136.91	-974.743	-1150.65	-3617.36
Mean (Profit)	365.661	294.933	267.102	135.19	-900.756

Table 5: Wilcoxon Paired Rank test on trading returns. This table provides p-value for the paired Wilcoxon Rank test, with the alternative hypothesis that the return generated using a model in the row names is greater than the return from a model in the column names. Panel A provides the result without accounting for transaction costs, and panel B after considering it.

A: Paired comparision of the trading returns (without transaction costs)				
	DQ	SNS	SQ	random
DNS	1.1e-05	1.8e-07	0.09	1.8e-135
DQ		0.18	1	5.2e-123
B: Paired comparision of the trading returns (with transaction costs)				
DNS	3.7e-08	1.2e-05	4.9e-11	9.5e-158
DQ		0.77	7.3e-05	2.4e-142

Table 6: Industry-wise performance comparison Pre-COVID, during COVID and Post-COVID. This table presents the mean return of the trading strategy across industries. All the 100 stocks in the sample are classified into 11 industries using the GICS classification. Column 'N' represents number of stocks in the particular industry, Pre-COVID column represents the mean return for the January - February, 2020 period, the COVID column represents the mean return for March 2020, and the Post-COVID column represents the mean return for the April-December, 2020 period.

	Industry	N	Pre-COVID	COVID	Post-COVID	Full Sample
1	COMMUNICATION	4	124.67	-71.44	237.55	192.98
2	Consumer Discretionary	12	114.22	510.75	-65.96	12.13
3	Consumer goods	9	49.73	-98.93	62.13	46.64
4	Energy	7	171.43	322.09	71.32	108.9
5	FINANCE	26	77.85	503.22	105.38	133.94
6	Healthcare	10	165.9	183.63	101.03	118.72
7	Industrials	7	132	315.29	92.23	117.44
8	Materials	16	95.82	756.29	95.09	150.31
9	Real Estate	1	-228.27	410.53	63.18	43.55
10	SOFTWARE	5	89.61	-89.74	107.33	87.96
11	Utilities	3	-24.29	650.97	29.69	72.47

Table 7: Regression results: source of trading profit. This table summarizes the results on the regression of the portfolio trading returns with respect to the relevant options Greeks other than delta and vega. In particular, the independent variables considered in our model are theta, rho, gamma, vomma and vanna of the portfolio. Additional controls include the size of the underlying stock measured by the logarithm of market capitalization as on January 1, 2020 (log(Mcap) along with industry and expiration date fixed effects. The results in first column ignore transaction costs, and those in the second column account for transaction costs (the bid-ask spread).

	Dependent variable:	
	Return	
	Results without transaction costs	Results with transaction costs
Gamma	0.002 (0.040)	−0.008 (0.026)
Rho	0.0003 (0.0005)	−0.001** (0.0003)
Theta	0.00003 (0.00005)	0.00004 (0.00003)
Vanna	0.002 (0.002)	−0.001 (0.002)
Vomma	−0.00004 (0.0001)	0.00003 (0.0001)
log(Mcap)	−0.202 (0.208)	−0.830*** (0.148)
Expiry: Feb	0.934 (0.970)	1.418** (0.682)
Expiry: March	2.317** (1.176)	7.693*** (0.850)
Expiry: April	0.666 (0.976)	2.914*** (0.689)
Expiry: May	0.034 (0.975)	0.960 (0.686)
Expiry: June	0.771 (0.971)	1.770*** (0.683)
Expiry: July	0.065 (0.972)	0.530 (0.681)
Expiry: August	−1.858* (0.970)	−0.805 (0.682)
Expiry: September	2.431** (0.970)	2.972*** (0.683)
Expiry: October	−0.214 (0.970)	−0.133 (0.682)
Expiry: November	0.806 (0.971)	1.231* (0.682)
Expiry: December	0.671 (0.972)	1.093 (0.682)
Observations	1,199	1,199
R^2	0.036	0.222
Adjusted R^2	0.014	0.204
F Statistic	44.280**	334.934***
Note:		*p<0.1; **p<0.05; ***p<0.01

Appendix A.

Table A.1: List of stock options with the industry details

Symbol	Name	Industry	Symbol	Name	Industry
RELIANCE	Reliance Industries	Energy	BIOCON	Biocon	Healthcare
TCS	Tata Consultancy Services	Software	GAIL	GAIL (India)	Energy
HDFCBANK	HDFC Bank	Finance	TATATEA	Tata Consumer Products	Cons. goods
HINDLEVER	Hindustan Unilever	Cons. goods	HINDALC0	Hindalco Industries	Materials
INFOSYSTCH	Infosys	Software	AUROPHARMA	Aurobindo Pharma	Healthcare
HDFC	Housing Development Finance Corporation	Finance	ADANIEXPO	Adani Enterprises	Industrials
KOTAKMAH	Kotak Mahindra Bank	Finance	MOTHERSUMI	Motherson Sumi Systems	Cons. Disc.
ICICIBANK	ICICI Bank	Finance	GUJAMBCEM	Ambuja Cements	Materials
BAJAUTOFIN	Bajaj Finance	Finance	CADILAHC	Cadila Healthcare	Healthcare
BHARTI	Bharti Airtel	Communication	MUTHOOTFIN	Muthoot Finance	Finance
ASIANPAINT	Asian Paints	Materials	LUPIN	Lupin	Healthcare
ITC	ITC	Cons. goods	MCDOWELLN	United Spirits	Cons. goods
HCLTECH	HCL Technologies	Software	JUBLFOOD	Jubilant Foodworks	Cons. goods
SBIN	State Bank of India	Finance	UNIPHOS	UPL	Materials
MARUTI	Maruti Suzuki India	Cons. Disc.	IGL	Indraprastha Gas	Energy
WIPRO	Wipro	Software	NMDC	NMDC	Materials
UTIBANK	Axis Bank	Finance	APOLLOHOSP	Apollo Hospitals Enterprise	Healthcare
LT	Larsen & Toubro	Industrials	HINDPETRO	Hindustan Petroleum Corporation	Energy
ULTRACEMCO	UltraTech Cement	Materials	NICOLASPIR	Piramal Enterprises	Finance
SUNPHARMA	Sun Pharmaceutical Industries	Healthcare	PNB	Punjab National Bank	Finance
BAJAJFINSV	Bajaj Finserv	Finance	SAIL	Steel Authority of India	Materials
TITAN	Titan Company	Cons. Disc.	ACC	ACC	Materials
ONGC	Oil & Natural Gas Corporation	Energy	PFC	Power Finance Corporation	Finance
DIVISLAB	Divi's Laboratories	Healthcare	BEL	Bharat Electronics	Industrials
BAJAJ_AUTO	Bajaj Auto	Cons. Disc.	BANKBARODA	Bank of Baroda	Finance
POWERGRID	Power Grid Corporation of India	Utilities	ASHOKLEY	Ashok Leyland	Cons. Disc.
NTPC	NTPC	Utilities	VOLTAS	Voltas	Cons. goods
MUNDRAPORT	Adani Ports and Special Economic Zone	Industrials	JINDALSTEL	Jindal Steel & Power	Materials
DABUR	Dabur India	Cons. goods	SRTRANSFIN	Shriram Transport Finance Company	Finance
TECHM	Tech Mahindra	Software	RECLTD	REC	Finance
JSWSTL	JSW Steel	Materials	TATAPOWER	Tata Power Company	Utilities
MM	Mahindra & Mahindra	Cons. Disc.	TVSSUZUKI	TVS Motor Company	Cons. Disc.
DRREDDY	Dr. Reddy's Laboratories	Healthcare	MMFIN	Mahindra & Mahindra Financial Services	Finance
BRITANNIA	Britannia Industries	Cons. goods	ZEETELE	Zee Entertainment Enterprises	Communication
IOC	Indian Oil Corporation	Energy	BATAINDIA	Bata India	Cons. goods
COALINDIA	Coal India	Materials	LTFH	L&T Finance Holdings	Finance
BPCL	Bharat Petroleum Corporation	Energy	CANBK	Canara Bank	Finance
TISCO	Tata Steel	Materials	LICHSGFIN	LIC Housing Finance	Finance
ICICIPRULI	ICICI Prudential Life Insurance Company	Finance	ESCORTS	Escorts	Cons. Disc.
EICHERMOT	Eicher Motors	Cons. Disc.	MANAPPURAM	Manappuram Finance	Finance
INDUSINDBK	IndusInd Bank	Finance	GLENMARK	Glenmark Pharmaceuticals	Healthcare
INDIGO	InterGlobe Aviation	Industrials	RBLBANK	RBL Bank	Finance
CIPLA	Cipla	Healthcare	FEDERALBNK	The Federal Bank	Finance
HEROHONDA	Hero MotoCorp	Cons. Disc.	BHEL	Bharat Heavy Electricals	Industrials
INFRATEL	0	Communication	TATACHEM	Tata Chemicals	Materials
GRASIM	Grasim Industries	Materials	IBULHSGFIN	Indiabulls Housing Finance	Finance
SESAGOA	Vedanta	Materials	APOLLOTYRE	Apollo Tyres	Cons. Disc.
DLF	DLF	Real Estate	NATIONALUM	National Aluminium Company	Materials
HAVELLS	Havells India	Industrials	PVR	PVR	Communication
TELCO	Tata Motors	Cons. Disc.	IDFCBANK	IDFC	Finance